JOURNAL OF GEOPHYSICAL RESEARCH, VOL. 113, A12307, doi:10.1029/2008JA013425, 2008

A method for the intensification of atomic oxygen green line emission by internal gravity waves

T. D. Kaladze,[1] W. Horton,[2,3] T. W. Garner,[3] J. W. Van Dam,[2] and M. L. Mays[2]

Received 27 May 2008; revised 26 August 2008; accepted 7 October 2008; published 18 December 2008.

[1] Low-frequency internal gravity waves, such as may be generated by seismic activity and nonlinearly propagated through the stably stratified atmosphere to the *E* layer of the ionosphere, are shown to cause intensification of atomic oxygen green line emission when their amplitude is sufficiently large. The nonlinear equations for the internal gravity waves are derived with the interaction of the induced currents with the geomagnetic field taken into account. When the source of the internal gravity waves is sufficiently strong, nonlinear vortex structures are predicted to be formed in the upper stratosphere and lower ionosphere. These nonlinear vortex structures are damped owing to Joule losses. The vortices provide a mechanism for increasing the concentration of atomic oxygen in the *E* layer and hence the associated intensity of the green light radiation at 557.7 nm. Data are discussed that report the observation of enhanced green light emission prior to earthquakes; this could lead to a forecasting model if the connection with seismic activity can be established.

Citation: Kaladze, T. D., W. Horton, T. W. Garner, J. W. Van Dam, and M. L. Mays (2008), A method for the intensification of atomic oxygen green line emission by internal gravity waves, *J. Geophys. Res.*, *113*, A12307, doi:10.1029/2008JA013425.

1. Introduction

[2] Acoustic gravity waves (AG) play an important role in a number of physical phenomena in the troposphere and in the dynamics of the ionospheric plasma. The main reason for the importance of studying AG waves, related to their practical applications, is that energy and momentum fluxes transported by AG waves from the lower to the upper ionosphere are comparable to or even larger than those coming from the solar wind or other sources [*Francis*, 1975; *Fritts et al.*, 1990; *Kim and Mahrt*, 1992; *Ebel*, 1984; *Alexander and Pfister*, 1995]. The gravity wave spectrum is an essential source of energy and momentum for the mesosphere and lower thermosphere, and couples the upper atmosphere (mesosphere and thermosphere) with the lower atmosphere (troposphere). Theoretical and experimental studies have shown that earthquakes, volcanic eruptions, tornadoes, thunderstorms, solar eclipses, solar terminators, jet flows, polar and equatorial electrojets, meteors, strong explosions, and powerful rockets launches can be sources for AG waves in the ionosphere [*Gossard and Hooke*, 1975; *Grigor'ev*, 1999; *Tolstoy and Lau*, 1971; *Richmond*, 1978; *Roettger*, 1981; *Fovell et al.*, 1992; *Igarashi et al.*, 1994; *Cole and Greifinger*, 1969; *Kato*, 1980; *Kanamori*, 2004].

[1] I. Vekua Institute of Applied Mathematics, Tbilisi State University, Tbilisi, Georgia.
[2] Institute for Fusion Studies, University of Texas at Austin, Austin, Texas, USA.
[3] Space and Geophysics Laboratory, Applied Research Laboratories, University of Texas at Austin, Austin, Texas, USA.

0148-0227/08/2008JA013425$09.00

[3] AG waves consist of a relatively high-frequency acoustic branch and a low-frequency internal gravity (IG) branch. IG waves have typical periods of 10^2 sec $\leq \tau <$ 1 day, wavelengths of $\lambda \approx 10$ km, and propagation velocities of $v_p \approx 30$ m/s. Various methods of measuring the parameters of the atmosphere indicate the presence of AG waves over a large range of heights extending from the troposphere to high altitudes $z \leq 500$ km. A very complete survey of the observations of these waves in the troposphere has been provided by *Gossard and Hooke* [1975]. The modern theory of small-amplitude AG waves in the Earth's atmosphere has been presented recently by *Grigor'ev* [1999].

[4] Gravity waves are gas-density oscillations in the stably stratified atmosphere, generally with both horizontal and vertical velocity components. For purely vertically propagating waves, the maximum frequency of oscillation occurs at the buoyancy frequency $N = \omega_g$, which is determined by the gravity g and the atmospheric gradient scale height H. For general wave number vectors k, the oscillation frequency is given by $N\cos(\theta_{kg})$, where θ_{kg} is the angle between the vertical g and k vectors. At very low frequencies corresponding to periods on the order of one day, the waves couple to Rossby waves driven by the Coriolis force.

[5] During the past decade, interest has greatly increased in electromagnetic and ionospheric phenomena caused by lithospheric processes that are related to earthquake precursors. Much of the data from observations confirms that, before and after earthquakes, there is increased wave activity in the atmosphere and ionosphere. General results from investigations on this subject were presented at conferences in Japan [*Hayakawa and Fujinawa*, 1994; *Hayakawa*,

1999] and in monographs and reviews [*Pulinets and Boyarchuk*, 2004; *Gokhberg et al.*, 1995; *Liperovsky et al.*, 2000]. In particular, the excitation of AG waves has been observed. An analysis of the data on pre-twilight night-sky luminescence shows that, before an earthquake, an increase occurs in the intensity of green radiation of neutral atomic oxygen at a wavelength of 557.7 nm. This emission arises from the $O(^1S\text{-}^1D)$ transition and has a radiating layer at heights of 85–110 km. This increase in radiation begins several hours before an earthquake [*Fishkova et al.*, 1985; *Toroshelidze and Fishkova*, 1988; *Mikhalev et al.*, 2001] and provides preliminary evidence for the presence of internal gravity waves or acoustic gravity waves.

[6] On the basis of the data available from observations and experiments [*Hayakawa and Fujinawa*, 1994; *Hayakawa*, 1999; *Pulinets and Boyarchuk*, 2004; *Gokhberg et al.*, 1995; *Liperovsky et al.*, 2000; *Fishkova et al.*, 1985; *Toroshelidze and Fishkova*, 1988; *Mikhalev et al.*, 2001], we hypothesize that, prior to an earthquake, the dynamics in the atmosphere develop according to the following scheme. Tectonic processes occurring in the Earth's crust generate Rayleigh waves, which propagate over the Earth's surface from the epicenter at supersonic velocities (about 3 km/s). These Rayleigh waves give rise to atmospheric-pressure disturbances by means of vertical pulsed action on the air [*Kanamori*, 2004; *Blanc*, 1985; *Row*, 1967]. AG waves propagate vertically, almost undamped, to a height of 110 km [*Grigor'ev*, 1999; *Houghton*, 1986] (their amplitude increases exponentially as the height increases) and give rise to collective motions in the form of AG vortices. Owing to the convective vortex motion, the density of atomic oxygen at these heights increases and, consequently, the intensity of green night-sky radiation is enhanced. The present paper is devoted to a theoretical justification of this model. In this connection, a problem of current interest is the theoretical study of whether the propagation of seismic disturbances can generate AG vortices in the stratosphere, mesosphere, and the lower ionosphere of the Earth.

[7] In the present paper we will focus our attention on how charged particles can influence the nonlinear propagation peculiarities of IG waves in the weakly ionized conductive ionospheric *E* layer. Also we will estimate the amplification of the night-sky green line intensity due to the damping of nonlinear IG vortices. In section 2, the basic equations are formulated. The reduced nonlinear equations for the IG waves with the Pedersen conductivity of the Earth's ionosphere taken into account are obtained in section 3, and the evolution of nonlinear solitary vortical structures in the conductive ionosphere is investigated. The increase in the intensity of green night-sky radiation is discussed in section 4. Conclusions are presented in section 5.

2. Basic Equations for Internal Gravity Waves

[8] The *E* layer dynamics is largely determined by its massive neutral particles, owing to the fast ion-neutral collision frequency $\nu_{\text{in}} \gg \omega$, where ω is the wave frequency for the internal gravity waves. The low-density ions, with density n, are embedded in a neutral gas with density N, where the density fraction n/N can be as high as 10^{-6}. However, the Lorenz force acting on the ions is of order 10^6 larger than the horizontal forces acting on the neutral gas, including the Coriolis force. Thus the horizontal acceleration is mostly due to the ion component of the system. In addition, the ion component makes the gas electrically conducting, and the ionospheric plasma is immersed in the geomagnetic field $\mathbf{B}_0$. Therefore, the interaction of the inductive current with the geomagnetic field must be taken into account.

[9] The propagation of IG waves under such conditions for the conductive ionosphere has not yet been studied properly. Hence in our investigation we must take into account the effects of the interaction of the induced ionospheric current with the geomagnetic field. A systematic investigation of the influence of charged particles in the ionosphere was first undertaken by *Kaladze and Tsamalashvili* [1997], *Kaladze* [1999], and *Kaladze et al.* [2004, 2008] in order to study nonlinear solitary vortex motions caused by planetary Rossby waves.

[10] Let us introduce a local Cartesian system of coordinates (x, y, z) with the x-axis directed from the west to the east, the y-axis from the south to the north, and the z-axis along the local upward-directed vertical. In such a system the dipole geomagnetic field is $\mathbf{B}_0(0, B_{0y}, B_{0z})$, and for the Earth's angular velocity we have $\mathbf{\Omega}_0(0, \Omega_{0y}, \Omega_{0z})$. For the IG waves we consider $\mathbf{B}_0$ and $\mathbf{\Omega}_0$ to be uniform. In this analysis we neglect the tilt of the magnetic dipole from the spin axis of the Earth.

[11] The dynamics of the electrically conducting ionospheric plasma can be described with the help of the momentum equation

$$\frac{d\mathbf{u}}{dt} \equiv \frac{\partial \mathbf{u}}{\partial t} + (\mathbf{u} \cdot \nabla)\mathbf{u} = -\frac{\nabla p}{\varrho} + \frac{1}{\varrho}\mathbf{j} \times \mathbf{B}_0 - 2\mathbf{\Omega}_0 \times \mathbf{u} + \mathbf{g}\,. \quad (1)$$

Here $\mathbf{j}$ is the electric current, $\mathbf{u}$ is the bulk (neutral) velocity, p and ϱ are the pressure and mass density of the medium respectively, and $\mathbf{g}(0, 0, -g)$ is the gravitational acceleration. In equation (1) the collisional drag force between the neutral gas and the ions has been replaced with the force balance equation for the ionized gas component, which introduces the $\mathbf{j} \times \mathbf{B}$ acceleration.

[12] The main purpose of the present study is to find the Lorentz force $\mathbf{j} \times \mathbf{B}_0$, since it significantly determines the specific character of the ionospheric dynamics (especially at high altitudes). The most important impact of this force is on the inductive damping in a conductive medium [*Cowling*, 1976]. For sufficiently large-scale motions we can neglect the viscous force in equation (1) relative to the Lorentz force [*Dokuchaev*, 1959].

[13] We consider the ionospheric plasma to be quasi-neutral and neglect the internal electrostatic electric field ($\mathbf{E} = -\nabla\varphi = 0$). Using the so-called non-inductive approximation [*Dokuchaev*, 1959], we find it is sufficient to consider the currents arising in the gas, whereas the vortex part of the self-generated electromagnetic field can be ignored. Assuming no external electric field and the ion and electron pressures to be small compared with that for neutrals, we find that the effective electric field in the generalized Ohm's law is equal to the dynamo field

[*Kaladze and Tsamalashvili*, 1997; *Kaladze*, 1999; *Kaladze et al.*, 2004, 2008], i.e.,

$$\mathbf{j} = \sigma_{\|}\mathbf{E}_{d\|} + \sigma_{\perp}\mathbf{E}_{d\perp} + \frac{\sigma_H}{B_0}\mathbf{B}_0 \times \mathbf{E}_d, \tag{2}$$

where

$$\sigma_{\|} = \frac{ne^2}{m_e \nu_e}, \tag{3}$$

$$\sigma_p = \sigma_{\perp} = \frac{ne^2\nu_{in}(\nu_e\nu_{in} + \omega_{ce}\omega_{ci})}{m_e\left(\omega_{ce}^2\nu_{in}^2 + \nu_e^2\nu_{in}^2 + \omega_{ce}^2\omega_{ci}^2\right)}, \tag{4}$$

$$\sigma_H = \frac{ne^2\nu_{in}^2\omega_{ce}}{m_e\left(\omega_{ce}^2\nu_{in}^2 + \nu_e^2\nu_{in}^2 + \omega_{ce}^2\omega_{ci}^2\right)}. \tag{5}$$

In equations (2)–(5) $\sigma_{\|}$, $\sigma_{\perp}$, and σ_H are the parallel (Cowling), perpendicular (Pedersen), and Hall conductivities, respectively. In equation (2) the subscripts $\|$ and $\perp$ denote components that are parallel and perpendicular to the external magnetic field. The quantities ν_{ne} and ν_{ni} are the effective collisional frequencies of the neutral particles with the electrons and ions, respectively; the meaning of the collisional frequencies ν_{ei} and ν_{en} is clear from their designations. Also, e is the absolute charge of the electrons; $\nu_e = \nu_{ei} + \nu_{en}$; and $\omega_{ce} = eB_0/m_e$ and $\omega_{ci} = ZeB_0/m_i$ are the electron and ion cyclotron frequencies. The electric field $\mathbf{E}_d = \mathbf{u} \times \mathbf{B}_0$ stands for the so-called dynamo field.

[14] To exclude the high-frequency acoustic mode, we make use of the incompressibility condition

$$\nabla \cdot \mathbf{u} = 0. \tag{6}$$

Then we supplement equation (1) by the following continuity equation for the total density ($\varrho = \varrho_0 + \tilde{\varrho}$)

$$\frac{d\varrho}{dt} = \frac{\partial \varrho}{\partial t} + (\mathbf{u}\cdot\nabla)\varrho = 0. \tag{7}$$

[15] The background mass density is stratified by the gravitational field. In the thermosphere it varies as

$$\varrho_0(z) = \varrho(0)\exp\left(-\frac{z}{H}\right), \tag{8}$$

where $H = c_s^2/\gamma g = k_B T/\langle m\rangle\, g$ is the reduced atmospheric height, γ is the ratio of specific heats, and c_s is the sound velocity. For an isothermal atmosphere $\gamma = 1$ and the relations are clear.

[16] Let us now consider the ionospheric E layer that is situated at heights of 85–110 km surface. The plasma conditions in this region ($\nu_e \approx \nu_{en}$, $\nu_{in}\nu_{en} \ll \omega_{ce}\omega_{ci}$ and $\nu_{in} \gg \omega_{ci}$) allow us to simplify the expression for the inductive electric current. First, since $\omega_{ci} \ll \nu_{in}$, the ions can be considered as unmagnetized. It is well known that the ion velocity across the magnetic field coincides with the wind velocity [see, e.g., *Kaladze et al.*, 2004], i.e., $\mathbf{v}_i = \mathbf{v}$, and thus the ions are completely dragged by the ionospheric winds. However, the electrons are magnetized, $\omega_{ce} \gg \nu_{en}$, and thus they are frozen in the external magnetic field. In this limiting case the Hall conductivity is $\sigma_H \approx en/B_0$, whereas the Pedersen conductivity is $\sigma_p \approx \sigma_H\omega_{ci}/\nu_{in} \ll \sigma_H$ (see equations (4) and (5)). For a numerical estimate we use the typical values $n/N \sim 10^{-8}$–10^{-6}, $\nu_{ei} \sim 10^3\ \mathrm{s}^{-1}$, $\nu_{en} \sim 10^4\ \mathrm{s}^{-1}$, $\nu_{in} \sim 10^3\ \mathrm{s}^{-1}$, $\omega_{ce} \sim 10^7\ \mathrm{s}^{-1}$, $\omega_{ci} \sim 3 \times 10^2\ \mathrm{s}^{-1}$, $\sigma_H \approx 3 \times 10^{-4}$ S/m and $\sigma_p \approx 10^{-4}$ S/m. The ratio of the magnetic term to the Coriolis term depends on the degree of ionization $n/N = mn/\varrho_0$. For the E layer the value $enB_0/\varrho_0 \approx (n/N)\omega_{ci} \approx 10^{-4}\ \mathrm{s}^{-1}$ is comparable to $2\Omega_0 \sim 10^{-4}$ rad/s. In addition we consider the ratio n/ϱ_0 to be independent of height z [*Gershman*, 1974]. As the characteristic frequency of IG waves ($\omega \sim 10^{-2}$ rad/s) is sufficiently high, we may conclude that both the Coriolis force and the Lorentz force caused by the Hall conductivity have negligibly small influence on the propagation properties of IG waves. As for the Pedersen conductivity contribution, it is well known [*Cowling*, 1976; *Dokuchaev*, 1959] that it appears as inductive (magnetic) inhibition and stipulates Joule damping of IG waves.

[17] Thus, the momentum equation for our case of interest is

$$\frac{d\mathbf{u}}{dt} = -\frac{\nabla p}{\varrho} - \frac{\sigma_p B_0^2}{\varrho}\mathbf{u}_{\perp} + \mathbf{g}, \tag{9}$$

where

$$\mathbf{u}_{\perp} = \mathbf{u} - \mathbf{B}_0\frac{(\mathbf{u}\cdot\mathbf{B}_0)}{B_0^2} \tag{10}$$

is the velocity component perpendicular to the geomagnetic field.

[18] Further simplification of the momentum equation is connected with the fact that the density variation in the internal gravity waves does not exceed 3–4% [*Miropol'sky*, 1981]. Hence the ratio of the perturbed to unperturbed density is $\frac{\tilde{\varrho}}{\varrho_0} \simeq (1\text{–}4) \times 10^{-2}$. For this reason, in the momentum equation, equation (9), we neglect $\tilde{\varrho}$ compared with $\varrho_0(z)$ for the inertial and Coriolis force terms and use the *Boussinesq* approximation to obtain the following expression:

$$\varrho_0(z)\frac{d\mathbf{u}}{dt} = -\nabla p + \varrho\mathbf{g} - \sigma_p B_0^2\mathbf{u}_{\perp}. \tag{11}$$

[19] Thus equations (7) and (11) constitute the initial set of equations with which to investigate the propagation dynamics of IG waves in the weakly ionized ionospheric E layer.

3. Nonlinear Dynamics of Internal Gravity Waves

3.1. Reduction of the Nonlinear Equations

[20] The nonlinear properties of small-amplitude AG waves have been considered by many authors [see, e.g., *Miropol'sky*, 1981; *Yeh and Liu*, 1981; *Weinstock*, 1984]. Reduced nonlinear equations describing the propagation dynamics of AG solitary structures have also been obtained

by *Stenflo* [1987, 1990, 1996]. Although such equations with vector nonlinearities are useful in the theory of neutral atmospheric motion, they must be improved for motion in the conductive ionosphere because they do not take into account the influence of electromagnetic forces. In what follows we will obtain reduced nonlinear equations for the internal gravity waves with the conductivity of the Earth's ionosphere taken into account.

[21] To investigate the nonlinear dynamics of low-frequency incompressible internal gravity waves, we consider two-dimensional motion in the (x-z) plane, assuming $\mathbf{u}(u, 0, w)$, $\mathbf{B}_0(0, B_{0y}, B_{0z})$, and $\frac{\partial}{\partial y} = 0$. The notations and the coordinate system are the same as in the preceding section. We obtain from equation (11) the following system:

$$\varrho_0(z)\left(\frac{\partial u}{\partial t} + u\frac{\partial u}{\partial x} + w\frac{\partial u}{\partial z}\right) = -\frac{\partial p}{\partial x} - \sigma_{\mathrm{p}} B_0^2 u, \qquad (12)$$

$$\varrho_0(z)\left(\frac{\partial w}{\partial t} + u\frac{\partial w}{\partial x} + w\frac{\partial w}{\partial z}\right) = -\frac{\partial p}{\partial z} - \varrho g - \sigma_{\mathrm{p}} B_{0y}^2 w. \qquad (13)$$

After differentiating equation (12) with respect to z and equation (13) with respect to x and then subtracting one from the other and taking into account equation (6), we obtain

$$\varrho_0\left(\frac{\partial \zeta}{\partial t} + u\frac{\partial \zeta}{\partial x} + w\frac{\partial \zeta}{\partial z}\right) + \frac{d\varrho_0}{dz}\left(\frac{\partial u}{\partial t} + u\frac{\partial u}{\partial x} + w\frac{\partial u}{\partial z}\right) = g\frac{\partial \varrho}{\partial x} - u\frac{\partial}{\partial z}\left(\sigma_{\mathrm{p}} B_0^2\right) - \sigma_{\mathrm{p}} B_0^2 \frac{\partial u}{\partial z} + \sigma_{\mathrm{p}} B_{0y}^2 \frac{\partial w}{\partial x}. \qquad (14)$$

[22] Here the y-component of vorticity ζ is introduced:

$$\zeta = \frac{\partial u}{\partial z} - \frac{\partial w}{\partial x}. \qquad (15)$$

The condition of equation (6) allows us to introduce the stream function ψ in the following manner:

$$u = -\frac{\partial \psi}{\partial z}, \qquad w = \frac{\partial \psi}{\partial x}. \qquad (16)$$

Then the vorticity of equation (15) is given by $\zeta = -(\frac{\partial^2}{\partial x^2} + \frac{\partial^2}{\partial z^2})\psi = -\psi$, where is the two-dimensional Laplacian. Thus we find that equations (7) and (14) given in terms of ψ are as follows:

$$\varrho_0\left[\frac{\partial}{\partial t}\triangle\psi + J(\psi, \triangle\psi)\right] = -g\frac{\partial \tilde{\varrho}}{\partial x} - \frac{d\varrho_0}{dz}\left[\frac{\partial}{\partial t}\left(\frac{\partial \psi}{\partial z}\right) + J\left(\psi, \frac{\partial \psi}{\partial z}\right)\right] - \frac{\partial}{\partial z}\left(\sigma_{\mathrm{p}} B_0^2\right)\frac{\partial \psi}{\partial z} - \left(\sigma_{\mathrm{p}} B_0^2\right)\frac{\partial^2 \psi}{\partial z^2} - \left(\sigma_{\mathrm{p}} B_{0y}^2\right)\frac{\partial^2 \psi}{\partial x^2}, \qquad (17)$$

$$\frac{\partial \tilde{\varrho}}{\partial t} + \frac{\partial \psi}{\partial x}\frac{d\varrho_0}{dz} + J(\psi, \tilde{\varrho}) = 0. \qquad (18)$$

We have introduced the Jacobian $J(a, b) = \frac{\partial a}{\partial x}\frac{\partial b}{\partial z} - \frac{\partial a}{\partial z}\frac{\partial b}{\partial x}$.

[23] We find the solution of equations (17) and (18) in the following form for the standard isothermal atmosphere:

$$\psi = \bar{\psi}\exp\left(\frac{z}{2H}\right), \qquad \tilde{\varrho} = \bar{\varrho}\exp\left(-\frac{z}{2H}\right). \qquad (19)$$

[24] From equations (17) and (18), we obtain the following system:

$$\frac{\partial \triangle\bar{\psi}}{\partial t} - \frac{1}{4H^2}\frac{\partial \bar{\psi}}{\partial t} + \exp\left(\frac{z}{2H}\right)\left[\frac{1}{2H}\triangle\bar{\psi}\frac{\partial \bar{\psi}}{\partial x} - \frac{1}{2H}\bar{\psi}\frac{\partial \triangle\bar{\psi}}{\partial x} + J\left(\bar{\psi}, \triangle\bar{\psi}\right)\right] = -\frac{g}{\varrho_0}\frac{\partial \bar{\varrho}}{\partial x}\exp\left(-\frac{z}{2H}\right) - \frac{\sigma_{\mathrm{p}} B_0^2}{\varrho_0}\left(\frac{\bar{\psi}}{4H^2} + \frac{1}{H}\frac{\partial \bar{\psi}}{\partial z} + \frac{\partial^2 \bar{\psi}}{\partial z^2}\right) - \frac{1}{\varrho_0}\frac{\partial}{\partial z}\left(\sigma_{\mathrm{p}} B_0^2\right)\left(\frac{\bar{\psi}}{2H} + \frac{\partial \bar{\psi}}{\partial z}\right) - \frac{\sigma_{\mathrm{p}} B_{0y}^2}{\varrho_0}\frac{\partial^2 \bar{\psi}}{\partial x^2}, \qquad (20)$$

$$\frac{\partial \bar{\varrho}}{\partial t} + \exp\left(\frac{z}{2H}\right)\left[J\left(\bar{\psi}, \bar{\varrho}\right) - \frac{1}{2H}\bar{\varrho}\frac{\partial \bar{\psi}}{\partial x} - \frac{1}{2H}\bar{\psi}\frac{\partial \bar{\varrho}}{\partial x}\right] = \frac{\varrho_0}{H}\frac{\partial \bar{\psi}}{\partial x}\exp\left(\frac{z}{H}\right). \qquad (21)$$

[25] For the nonlinear terms it is reasonable to consider $\exp\left(\frac{z}{2H}\right) \approx 1$, i.e., $k_z \gg 1/2H$ (sufficiently short wave limit). This means that the Jacobian is the most essential nonlinear term. Thus, in place of equations (20) and (21), we obtain the following system of equations:

$$\frac{\partial}{\partial t}\left(\triangle\bar{\psi} - \frac{1}{4H^2}\bar{\psi}\right) + J\left(\bar{\psi}, \triangle\bar{\psi}\right) = -\frac{g}{\varrho_0}\frac{\partial \bar{\varrho}}{\partial x}\exp\left(-\frac{z}{2H}\right) - \frac{\sigma_{\mathrm{p}} B_0^2}{\varrho_0}\left(\frac{\bar{\psi}}{4H^2} + \frac{1}{H}\frac{\partial \bar{\psi}}{\partial z} + \frac{\partial^2 \bar{\psi}}{\partial z^2}\right) - \frac{1}{\varrho_0}\frac{\partial}{\partial z}\left(\sigma_{\mathrm{p}} B_0^2\right)\left(\frac{\bar{\psi}}{2H} + \frac{\partial \bar{\psi}}{\partial z}\right) - \frac{\sigma_{\mathrm{p}} B_{0y}^2}{\varrho_0}\frac{\partial^2 \bar{\psi}}{\partial x^2}, \qquad (22)$$

$$\frac{\partial \bar{\varrho}}{\partial t} + J\left(\bar{\psi}, \bar{\varrho}\right) = \frac{\varrho_0}{H}\frac{\partial \bar{\psi}}{\partial x}\exp\left(\frac{z}{H}\right). \qquad (23)$$

[26] Furthermore we assume the density profile to have the form $\varrho_0(z) = \varrho_0(0)\exp(-z/H)$ distribution (see equation (8)) and introduce the new variable $\chi = g\bar{\varrho}/\varrho_0(0)$. Under the assumption that $\sigma_{\mathrm{p}} B_{0y}^2/\varrho_0$ is constant along the z-axis [see, e.g., *Gershman*, 1974], we obtain

$$\frac{\partial}{\partial t}\left(\triangle\bar{\psi} - \frac{1}{4H^2}\bar{\psi}\right) + J\left(\bar{\psi}, \triangle\bar{\psi}\right) = -\frac{\partial \chi}{\partial x} - \frac{\sigma_{\mathrm{p}} B_0^2}{\varrho_0}\left(\frac{\partial^2 \bar{\psi}}{\partial z^2} - \frac{1}{4H^2}\bar{\psi}\right) - \frac{\sigma_{\mathrm{p}} B_{0y}^2}{\varrho_0}\frac{\partial^2 \bar{\psi}}{\partial x^2}, \qquad (24)$$

$$\frac{\partial \chi}{\partial t} + J\left(\bar{\psi}, \chi\right) = \omega_{\mathrm{g}}^2\frac{\partial \bar{\psi}}{\partial x}. \qquad (25)$$

In equation (25), the quantity $\omega_{\mathrm{g}} = (g/H)^{1/2} > 0$ is the Brunt-Väisälä frequency for the incompressible stably stratified

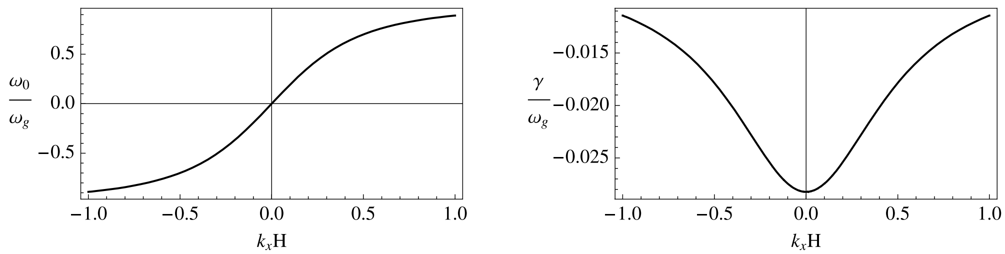

Figure 1. Plot of (left) equation (26) for the frequency and (right) equation (27) for the damping rate of the internal gravity wave in units of ω_g against k_xH for a scale height of H = 5 km.

atmosphere, often called N. Equations (24) and (25) lead to an eigenvalue problem that contains profiles of buoyancy and Pedersen conductivity. When the atmosphere is slowly varying in space over the scale of the structures (namely, the wavelength and the vortex size), the results from local and nonlocal analyses are equivalent. Strong spatial inhomogeneity of the wavelength would be necessary before the results change qualitatively. If the buoyancy frequency were to vary sharply, then the eigenvalue problem should be solved.

[27] Hence, the linear solution of equations (24) and (25) for the dispersion of internal gravity waves propagating zonally with small Pedersen conductivity is

$$\omega_0 = \pm \frac{k_x \omega_g}{\left(k_x^2 + k_z^2 + \frac{1}{4H^2}\right)^{1/2}}. \tag{26}$$

The damping rate γ is given by

$$\gamma = -\frac{\frac{\sigma_p B_{0y}^2}{\varrho_0} k_x^2 + \frac{\sigma_p B_0^2}{\varrho_0}\left(k_z^2 + \frac{1}{4H^2}\right)}{2\left(k_x^2 + k_z^2 + \frac{1}{4H^2}\right)}. \tag{27}$$

[28] The viscosity of air is $\nu_{air} \approx 1.5 \times 10^{-5}$ m^2/s and the damping rate is $k_x^2 \nu_{air} \approx 10^{-11}$ s^{-1} which is negligible compared with the Ohmic dissipation rate of $\gamma \approx \sigma_p B_0^2/\varrho_0 \approx 10^{-5}$ s^{-1}. The Hartmann number is $(\sigma_p B_0^2 H^2/\varrho_0 \nu_{air})^{1/2}$ which is of order 10^3 and higher. Thus the Ohmic damping is much faster than the viscous damping rate for vortex structures but is still long (several hours) compared to the rotation time of the vortex structures. For the typical E layer values given in section 5 the frequency and damping rate of the internal gravity wave (equations (26) and (27)) is shown in Figure 1 in units of ω_g against k_xH for a scale height of H = 5 km.

3.2. Vortex Solutions of the Reduced Nonlinear Equations

[29] The nonlinear behavior of the low-frequency AG perturbations is dominated by the presence of the convective derivative, and the corresponding vector-product nonlinearity can thus produce various coherent localized vortex structures for a broad range of background configurations. The forms of such vortices are strongly dependent on the spatial profile of the unperturbed medium. In a quiescent atmosphere with exponential density and pressure profiles, standard traveling dipolar vortices (also called AG modons) have been found, whose transverse dimensions are either much smaller than [*Stenflo*, 1987] or comparable to the density scale length [*Stenflo and Stepanyants*, 1995].

[30] The system of equations (24) and (25) describes the dynamics of nonlinear solitary vortices on the low-frequency internal gravity waves in the stably stratified ($\omega_g^2 > 0$) ionosphere of the Earth at sufficiently high latitudes. A solitary dipole vortex solution of equations (24) and (25) in a neutral ($\sigma_p = 0$) stably stratified atmosphere was found by *Stenflo and Stepanyants* [1995]. These vortex solutions describe rolls of gas about a horizontal axis, with gas moving from low to high altitudes over a vortex of diameter $2a$. An introduction to the physics of vortices in ionized gas is given by *Horton and Ichikawa* [1996].

[31] Let us introduce the normalized stream function

$$\chi = -\frac{\omega_g^2}{V}\bar{\psi}, \tag{28}$$

with the dipole vortex solutions, in the dissipationless limit of the nonlinear equations (24) and (25), given by

$$\bar{\psi}(r,\vartheta) = \begin{cases} \left[\frac{\lambda_i^2 Va}{\lambda_e^2 J_1\left(\frac{a}{\lambda_i}\right)} J_1\left(\frac{r}{\lambda_i}\right) - \left(\frac{\lambda_i}{\lambda}\right)^2 Vr\right] \cos\vartheta, & r < a, \\ -\frac{Va}{K_1\left(\frac{a}{\lambda_e}\right)} K_1\left(\frac{r}{\lambda_e}\right)\cos\vartheta, & r > a. \end{cases} \tag{29}$$

The polar coordinates $x - Vt = r \sin\vartheta$ and $z = r\cos\vartheta$ are introduced, where a is the last closed flux surface (or vortex half-diameter), V is the constant velocity of the structure, and the functions J_n and K_n are the standard Bessel and modified Bessel functions, respectively. Furthermore, we have

$$\lambda_e^{-2} = \frac{1}{4H^2} - \frac{\omega_g^2}{V^2}, \tag{30}$$

$$\lambda_i^{-2} = \left(\lambda^{-2} - \lambda^{-2}\right), \tag{31}$$

and the inequality $V^2 > 4H^2\omega_g^2$ is required. Thus the solution contains three parameters, λ, a and V, which have the following additional relationship:

$$\lambda_i \frac{J_2\left(\frac{a}{\lambda_i}\right)}{J_1\left(\frac{a}{\lambda_i}\right)} + \lambda_e \frac{K_2\left(\frac{a}{\lambda_e}\right)}{K_1\left(\frac{a}{\lambda_e}\right)} = 0. \tag{32}$$

[32] From equation (26) we conclude that the phase velocity $v_{ph} = \omega/k_x$ is bounded in the interval

$$-v_{max} \leq v_{ph} \leq v_{max}, \quad (33)$$

where $v_{max} = 2H\omega_g = 2(gH)^{1/2}$ in the case of an incompressible atmosphere. Thus, when a source is moving in the x-direction with a velocity larger than v_{max}, there is no resonance with internal gravity waves. The vortices propagate faster than the linear wave speeds owing to the nonlinear amplitude, as has been explained by *Horton and Ichikawa* [1996]. This means that such waves will not be generated by the source, i.e., there are no energy losses [*Stepanyants and Fabrikant*, 1992]. Therefore one can obtain a stationary solution for the localized nonlinear formation of a pulse propagating horizontally with a velocity $|V| > v_{max}$. We note that if we take $H \approx 4.5$–6 km as an estimate, we find $v_{max} \approx 500$ m/s. Thus, the nonlinear solitary vortex structure that forms should be supersonic and not decay owing to the generation of linear waves in the region $|V| < v_{max}$.

[33] Nonlinear pulses with amplitudes comparable to the vertical density scale length H are reported to propagate over distances of several horizontal wavelengths before dissipating [*Ramamurthy et al.*, 1990]. This suggests that nonlinear vortex structures like those considered here and by *Stenflo* [1991] for the stratosphere and E layer, may have been identified in the troposphere by *Ramamurthy et al.* [1990].

[34] In a general nonlinear state of the system there will be both a lower amplitude turbulent set of waves in the background and larger vortex and zonal flow structures. To make analytic progress in this work, we neglect the low amplitude background turbulence and consider only the solutions for the more energetic, large amplitude coherent structures made of vortices and flows. Chaotic states as given by *Yu* [1999] are expected when the amplitude of the pump waves becomes sufficiently large. We plan to study this problem of large-amplitude nonlinear interactions with the inclusion of "pump depletion effects" and onset of chaos in subsequent work.

3.3. Energy Conservation Relations

[35] In the mesosphere and stratosphere, the damping from viscosity is weak. In the E layer, however, the coupling to the weakly ionized plasma component leads to strong damping through the Pedersen conductivity. There are energy conservation relations for the exchange of kinetic flow energy and gravitational potential energy. To obtain the conservation relations we multiply equation (24) by $-\bar{\psi}$ and integrate over x and z. We obtain

$$\frac{1}{2}\frac{\partial}{\partial t}\int dxdz\left[(\nabla\bar{\psi})^2 + \frac{\bar{\psi}^2}{4H^2}\right] = -\int \chi\frac{\partial\bar{\psi}}{\partial x}dxdz - \frac{\sigma_P B_0^2}{\varrho_0}\int\left[\left(\frac{\partial\bar{\psi}}{\partial z}\right)^2 + \frac{\bar{\psi}^2}{4H^2}\right]dxdz - \frac{\sigma_P B_{0y}^2}{\varrho_0}\int\left(\frac{\partial\bar{\psi}}{\partial x}\right)^2 dxdz. \quad (34)$$

If we multiply equation (25) by χ, we obtain

$$\chi\frac{\partial\bar{\psi}}{\partial x} = \frac{1}{\omega_g^2}\left[\frac{1}{2}\frac{\partial\chi^2}{\partial t} + \chi J(\bar{\psi},\chi)\right]. \quad (35)$$

Integration of this equation over x and z leads to

$$\int \chi\frac{\partial\bar{\psi}}{\partial x}dxdz = \frac{1}{2\omega_g^2}\frac{\partial}{\partial t}\int \chi^2 dxdz. \quad (36)$$

The combined system of equations (34) and (36) gives the following energy dynamics law:

$$\frac{\partial E}{\partial t} = -\frac{\sigma_P B_{0y}^2}{\varrho_0}\int\left(\frac{\partial\bar{\psi}}{\partial z}\right)^2 dxdz - \frac{\sigma_P B_0^2}{\varrho_0}\int\left[\left(\frac{\partial\bar{\psi}}{\partial z}\right)^2 + \frac{\bar{\psi}^2}{4H^2}\right]dxdz, \quad (37)$$

where

$$E = \int dxdz\left[\frac{1}{2}(\nabla\bar{\psi})^2 + \frac{\bar{\psi}^2}{8H^2} + \frac{\chi^2}{2\omega_g^2}\right] \quad (38)$$

is the energy of the nonlinear solitary vortex dipole structure of the internal gravity waves. An interesting finding is that Joule dissipation, although it damps the vortex motion, which can contain a large amount of energy, heats the E layer. Physically, the atmospheric wave or vortex travels to E region altitudes, where the neutrals drag the ions across magnetic field lines. The wave loses energy as it pushes the ions across magnetic field lines.

[36] Thus, we conclude that the energy of the solitary vortex dipole structure of internal gravity waves is decreasing owing to Ohmic losses. The damping rate of such solitary vortex structures remains typically the same as for linear waves (see equation (27)).

4. Increase in the Intensity of Green Night-Sky Radiation

[37] The main source of excitation of green night-sky luminescence (λ = 557.7 nm) at heights from 80 to 120 km is the two-stage Bart-Hildebrant mechanism, which consists of the following reactions [*Slanger et al.*, 2001]:

$$\begin{aligned} O(^3P) + O(^3P) + M &= O_2^* + M, \\ O_2^* + O(^3P) &\longrightarrow O_2 + O(^1S), \end{aligned} \quad (39)$$

These are followed by the emission of the oxygen green line via the reaction

$$O(^1S) \longrightarrow O(^1D) + h\nu_0, \quad (40)$$

where $O(^3P)$ is atomic oxygen in the ground state, O_2^* is molecular oxygen in the excited state, M is any neutral particle, $O(^1S)$ and $O(^1D)$ are oxygen atoms in excited states, and ν_0 is the green line frequency. The radiation intensity I depends strongly on the concentration of atomic oxygen $n(O)$ in the radiating layer [*Toroshelidze and Fishkova*, 1988]:

$$I \sim \left(\frac{T_0}{300}\right)^{-2.9} n^3(O). \quad (41)$$

[38] To elucidate the role of induction damping of IG waves, we rewrite equations (12) and (13) in polar coordinates, $z = r \cos \vartheta$ and $x = r \sin \vartheta$:

$$\frac{du_r}{dt} = -\frac{1}{\varrho_0}\frac{\partial p}{\partial r} + \frac{\varrho}{\varrho_0} g_r - \frac{\sigma_p B_0^2}{\varrho_0} u_r, \quad (42)$$

$$\frac{du_\vartheta}{dt} = -\frac{1}{\varrho_0}\frac{\partial p}{r\partial\vartheta} + \frac{\varrho}{\varrho_0} g_\vartheta - \frac{\sigma_p B_0^2}{\varrho_0} u_\vartheta. \quad (43)$$

Considering a stationary case and assuming that the pressure in the azimuth direction is compensated by the gravitational action from equation (43), we obtain

$$v_r = -\frac{\sigma_p B_0^2}{2\varrho_0} r. \quad (44)$$

It is clear that the induction damping force creates a radial component of velocity that is directed to the center of vortex rotation, i.e., substance influx takes place. Thus, in the case of vortex motion in the ionospheric *E* layer, an increase of the particle concentration is possible owing to the induction damping.

[39] The variations of $n(O)$ at a height of ~100 km may be associated with the occurrence of IG vortices (28)–(33), which cause convective mixing of oxygen in the vertical direction and consequently increase the concentration $n(O)$ in the radiating atmospheric layer. Let us estimate how the concentration of the atomic oxygen $n(O)$ increases owing to IG vortices in the radiating layer ($z \sim 100$ km). In accordance with the definition of χ and equations (28) and (29), we obtain

$$\frac{\bar{\varrho}}{\varrho_0} = -\frac{\omega_g^2}{Vg}\bar{\psi} \sim a\frac{\omega_g^2}{g} > 0, \quad (45)$$

where $\bar{\varrho}$ is the variation in the density of atomic oxygen due to vortical convection. We see that, owing to such convection, the total density is increasing. Taking into account that $\varrho_0 = m(O)n(O)$ is the mass density of neutral oxygen and the total density is $\varrho = \varrho_0 + \bar{\varrho}$, from equations (41) and (45) we obtain

$$\frac{I_{obs}}{I_{seas}} \sim \left(\frac{\varrho}{\varrho_0}\right)^3 \sim \left(1 + a\frac{\omega_g^2}{g}\right)^3. \quad (46)$$

Here, I_{obs} and I_{seas} are the observed intensity and the seasonally averaged intensity, respectively.

[40] *Fishkova et al.* [1985], *Toroshelidze and Fishkova* [1988], and *Mikhalev et al.* [2001] argue, on the basis of long-term observations, that variations in the intensity of the main kinds of radiation in the atmosphere may possibly be a precursor for earthquakes when there is sufficient precursor tectonic activity to launch large amplitude gravity waves into the atmosphere. This study suggests tectonic plate motion studies need be used to estimate their effectiveness in terms of an effective antenna for converting seismic energy into gravity wave energy in the atmosphere. This effect is most pronounced in variations in green night radiation of atomic oxygen; its radiating layer is localized at a height of about 100 km. The difference $I = I_{obs} - I_{seas}$ was analyzed. It was found that, 24 hours before earthquakes, the intensity of the emission $\lambda = 557.7$ nm begins to increase. The amplitude I/I_{seas}, expressed in percentage, is 6.9 ± 1.4%.

[41] For a comparison with the observed intensity, by using equation (46) we determine the relative variation in the intensity I/I_{seas} of green radiation due to IG vortices:

$$\frac{\triangle I}{I_{seas}} \sim \left(1 + a\frac{\omega_g^2}{g}\right)^3 - 1 \quad (47)$$

where a is the radius of the vortex with a horizontal roll axis. We now perform some estimates. As the size a of the structures must be less than H, for estimation we may take $a \sim H/3$. For typical values of the atmospheric parameters $H \simeq 6 \cdot 10^3$ m, $\omega_g \simeq 10^{-2}$ s^{-1}, $g \sim 10$ m/s^2, in accordance with (47), we obtain $I/I_{seas} \simeq 6\%$. Thus the observed variations in the intensity (before earthquakes) I/I_{seas} could be measured.

[42] Hence, the observed variations in the emission at $\lambda = 557.7$ nm, which are related to enhanced seismic activity, are quantitatively consistent with the proposed theory of the propagation of IG vortices in the middle atmosphere.

5. Discussion

[43] The purpose of the present paper is to propose a theoretical explanation for an increase in the intensity of green radiation of atomic oxygen at a wavelength of $\lambda = 557.7$ nm (the radiating layer at ionospheric *E* layer heights) observed before earthquakes. To this end we have considered the propagation peculiarities of internal-gravity waves in the Earth's weakly ionized conductive ionosphere.

[44] IG waves are the low-frequency branch of acoustic-gravity (AG) waves. IG waves have typical frequency $\omega \sim 10^{-2}$ s^{-1} and wavelength $\lambda \approx 10$ km. They propagate with velocities $v_p \sim 10-100$ m/s. In addition, all perturbed velocity components increase with height, while the pressure and density decrease. According to observations, IG waves exist in a large range of heights extending from the troposphere to $z \leq 500$ km. At such heights the Earth's ionosphere is conductive owing to the presence of charged particles.

[45] The basic equations that incorporate both electromagnetic and Coriolis forces were discussed in section 2. Using the noninductive approximation we considered the current arising in the gas but neglected the vortex parts of the self-generated electromagnetic field. Thus, only the dynamo electric field was taken into account. The ionospheric gas was assumed to be vertically stably stratified, and we considered an isothermal atmosphere for the adiabatically propagating IG perturbations.

[46] Owing to the relatively high frequency of the IG waves, the influence of the Coriolis and Lorentz forces caused by the Hall conductivity is negligibly small, while the Pedersen conductivity arises from inductive (magnetic) inhibition and leads to Joule damping of IG waves. We calculated the corresponding damping rate (see equation (27)). For the typical E layer values $\sigma_p \cong 10^{-4}$ S/m, $\rho_0 = 10^{-10}$ kg/m^3, $B_0 = 0.5 \times 10^{-4}$ T, we obtained $\gamma \sim 10^{-3}$ s^{-1} for the damping rate. Thus linear IG waves freely propagating through the atmosphere undergo strong damping due to Joule losses in the E layer.

[47] In section 3 we investigated the nonlinear propagation of internal-gravity waves in the conductive ionosphere of the Earth. We obtained a simplified set of two-dimensional equations for the dynamics of IG waves in the conductive stably stratified ionosphere. A major finding of this research was to show how the influence of the conductivity of the Earth's ionosphere influences the horizontal vortex rolls, which bring higher densities of the lower atomic oxygen up into the ionosphere. Here they are indirectly excited to emit enhanced levels of green light with large energy releases from the surface of the Earth, rather than by enhanced electron precipitation (as in an auroral display). We noted that there are preliminary data showing a correlation of enhanced green light emission with tectonic activity. In particular, we considered nonlinear solitary vortex structures that are formed on the internal gravity waves. Vortex structures deserve attention because they carry along the trapped medium particles and thus make an essential contribution to transport phenomena. In addition we showed that the vortex motions may be used to explain some natural phenomena that occur prior to earthquakes. We obtained basic nonlinear equations for the two-dimensional (in x-z plane) IG wave motions taking into account the Pedersen conductivity of the ionosphere. In the absence of Ohmic conductivity we obtained nonlinear equations that describe the propagation of solitary dipolar vortex structures. We obtained the dynamical evolution equation for the energy of solitary vortex structures on IG waves (see equation (37)). We showed that the energy of solitary dipolar vortex structure on IG waves is damped owing to Ohmic losses. The damping rate of such solitary vortex structures is the same as that for linear waves (see equation (27)).

[48] We showed that seismic-origin IG disturbances propagating from the lower atmospheric layers with almost no damping reach heights of $\sim$110 km, where strongly localized IG vortices are formed. Vortex structures entrain neutral particles and can travel with them either toward the east or the west. Under the action of disturbances, they can also move upward and downward.

[49] We showed that the damping of vortex structures causes a radial influx of neutrals and increases the neutral density in the atmosphere at this height. The increase in the density of oxygen atoms increases the efficiency of their recombination and consequently enhances the intensity of green night-sky radiation.

[50] We estimated the fluctuations in the density of the atomic oxygen, which are caused by IG vortices, and the corresponding increase in the intensity of green night-sky luminescence. A comparison of the theoretical estimate for the increase in the intensity of the green line with data from observations conducted before strong earthquakes shows there may be a significant correlation. Research establishing the degree of correlation will require further work.

[51] We conclude that the variations in the radiation at λ = 557.7 nm during periods of seismic activity might be caused by the generation of IG vortices in the middle atmosphere; hence, they can be considered to be an immediate (24–48 hours) indicator of earthquakes.

[52] **Acknowledgments.** The research described in this publication was made possible in part by award GEP2-3340-TB-06 of the Georgian Research and Development Foundation (GRDF) and the U.S. Civilian Research and Development Foundation for the Independent States of the Former Soviet Union (CRDF)), and NSF grant ATM-0638480 to The University of Texas at Austin.

[53] Amitava Bhattacharjee thanks the reviewers for their assistance in evaluating this paper.

References

Alexander, M. J., and L. Pfister (1995), Gravity wave momentum flux in the lower stratosphere over convection, *Geophys. Res. Lett.*, *22*(15), 2029–2032.

Blanc, E. (1985), Observations in the upper atmosphere of infrasonic waves from natural or artificial sources—A summary, *Ann. Geophys.*, *3*, 673–687.

Cole, J. D., and C. Greifinger (1969), Acoustic-gravity waves from an energy source at the ground in an isothermal atmosphere, *J. Geophys. Res.*, *74*(14), 3693–3703.

Cowling, T. G. (1976), *Magnetohydrodynamics, Monographs on Astronomical Subjects*, Hilger, Bristol, U. K.

Dokuchaev, V. P. (1959), Influence of the Earth's magnetic field on the ionospheric winds, *Izv. Akad. Nauk SSSR, Ser. Fiz.*, *5*, 783.

Ebel, A. (1984), Contributions of gravity waves to the momentum, heat and turbulent energy budget of the upper mesosphere and lower thermosphere, *J. Atmos. Terr. Phys.*, *46*, 727–737.

Fishkova, L. M., M. B. Gokhberg, and V. A. Pilipenko (1985), Relationship between night airglow and seismic activity, *Ann. Geophys.*, *3*, 689–694.

Fovell, R., D. Durran, and J. R. Holton (1992), Numerical simulations of convectively generated stratospheric gravity waves, *J. Atmos. Sci.*, *49*, 1427–1442.

Francis, S. H. (1975), Global propagation of atmospheric gravity waves—A review, *J. Atmos. Terr. Phys.*, *37*, 1011–1054.

Fritts, D. C., T. Tsuda, T. E. VanZandt, S. A. Smith, T. Sato, S. Fukao, and S. Kato (1990), Studies of velocity fluctuations in the lower atmosphere using the MU radar. Part II: Momentum fluxes and energy densities, *J. Atmos. Sci.*, *47*, 51–66.

Gershman, B. N. (1974), *Dynamics of the Ionospheric Plasma*, Nauka, Moscow.

Gokhberg, M. B., V. A. Morgounov, and O. A. Pokhotelov (1995), *Earthquake Prediction: Seismo-electromagnetic Phenomena*, Gordon and Breach, Reading, Pa.

Gossard, E. E., and W. H. Hooke (1975), *Waves in the Atmosphere*, Elsevier, Amsterdam.

Grigor'ev, G. I. (1999), Acoustic-gravity waves in the Earth's atmosphere (review), *Radiophys. Quantum Electron.*, *42*, 1–21.

Hayakawa, M. (1999), *Atmospheric and Ionospheric Electromagnetic Phenomena Associated With Earthquakes*, Terra Sci., Tokyo.

Hayakawa, M., and Y. Fujinawa (1994), *Electromagnetic Phenomena Related to Earthquake Prediction*, Terra Sci., Tokyo.

Horton, W., and Y. Ichikawa (1996), *Chaos and Structures in Nonlinear Plasmas*, World Sci., Hackensack, N. J.

Houghton, J. T. (1986), *The Physics of Atmospheres*, 2nd ed., Cambridge University Press, Cambridge, U. K.

Igarashi, K., S. Kainuma, I. Nishimuta, S. Okamoto, H. Kuroiwa, T. Tanaka, and T. Ogawa (1994), Ionospheric and atmospheric disturbances around Japan caused by the eruption of Mount Pinatubo on 15 June 1991, *J. Atmos. Terr. Phys.*, *56*, 1227–1234.

Kaladze, T. D. (1999), Magnetized Rossby waves in the Earth's ionosphere, *Plasma Phys. Rep.*, *25*, 284–287.

Kaladze, T. D., and L. V. Tsamalashvili (1997), Solitary dipole vortices in the Earth's ionosphere, *Phys. Lett. A*, *232*, 269–274.

Kaladze, T. D., G. D. Aburjania, O. A. Kharshiladze, W. Horton, and Y.-H. Kim (2004), Theory of magnetized Rossby waves in the ionospheric *E* layer, *J. Geophys. Res.*, *109*, A05302, doi:10.1029/2003JA010049.

Kaladze, T. D., O. A. Pokhotelov, H. A. Shah, M. I. Khan, and L. Stenflo (2008), Acoustic-gravity waves in the Earth's ionosphere, *J. Atmos. Sol. Terr. Phys.*, *70*, 1607–1616, doi:10.1016/j.jastp.2008.06.009.

Kanamori, H. (2004), Some fluid-mechanical problems in geophysics: Waves in the atmosphere and fault lubrication, *Fluid Dyn. Res.*, *34*, 1–19.

Kato, S. (1980), *Dynamics of the Upper Atmosphere*, Cent. for Acad. Publ. Jpn., Tokyo.

Kim, J., and L. Mahrt (1992), Momentum transport by gravity waves, *J. Atmos. Sci.*, *49*, 735–748.

Liperovsky, V. A., O. A. Pokhotelov, E. V. Liperovskaya, M. Parrot, C.-V. Meister, and O. A. Alimov (2000), Modification Of sporadic E-layers caused by seismic activity, *Surv. Geophys.*, *21*, 449–486.

Mikhalev, A. V., M. S. Popov, and E. S. Kazimirovsky (2001), The manifestation of seismic activity in 557.7 nm emission variations of the Earth's upper atmosphere, *Adv. Space Res.*, *27*, 1105–1108.

Miropol'sky, Y. Z. (1981), *Dynamics of Internal Gravity Waves in the Ocean*, Gidrometeoizdat, Leningrad, Russia.

Pulinets, S., and K. Boyarchuk (2004), *Ionospheric Precursors of Earthquakes*, Springer, New York.

Ramamurthy, M. K., B. P. Collins, R. M. Rauber, and P. C. Kennedy (1990), Evidence of very-large-amplitude solitary waves in the atmosphere, *Nature*, *348*, 314–317, doi:10.1038/348314a0.

Richmond, A. D. (1978), Gravity wave generation, propagation, and dissipation in the thermosphere, *J. Geophys. Res.*, *83*, 4131–4145.

Roettger, J. (1981), Equatorial spread-F by electric fields and atmospheric gravity waves generated by thunderstorms, *J. Atmos. Terr. Phys.*, *43*, 453–462.

Row, R. V. (1967), Acoustic-gravity waves in the upper atmosphere due to a nuclear detonation and an earthquake, *J. Geophys. Res.*, *72*, 1599–1610.

Slanger, T. G., P. C. Cosby, D. L. Huestis, and T. A. Bida (2001), Discovery of the atomic oxygen green line in the Venus night airglow, *Science*, *291*, 463–465.

Stenflo, L. (1987), Acoustic solitary vortices, *Phys. Fluids*, *30*, 3297–3299.

Stenflo, L. (1990), Acoustic gravity vortices, *Phys. Scr.*, *41*, 641–642.

Stenflo, L. (1991), Acoustic gravity vortices in the atmosphere, *Z. Naturforsch.*, *46a*, 560.

Stenflo, L. (1996), Nonlinear equations for acoustic gravity waves, *Phys. Lett. A*, *222*, 378–380.

Stenflo, L., and Y. A. Stepanyants (1995), Acoustic-gravity modons in the atmosphere, *Ann. Geophys.*, *13*, 973–975.

Stepanyants, Y. A., and A. L. Fabrikant (1992), Features of the Cherenkov emission of drift waves in hydrodynamics and in a plasma, *Sov. Phys. JETP, Engl. Transl.*, *75*, 818.

Tolstoy, I., and J. Lau (1971), Generation of long internal gravity waves in waveguides by rising buoyant air masses and other sources, *Geophys. J. Roy. Astron. Soc.*, *26*, 295–310.

Toroshelidze, T. I., and L. M. Fishkova (1988), Analysis of fluctuations of the nightglow of the middle and upper atmosphere preceding earthquakes, *Dokl. Akad. Nauk SSSR*, *302*, 313–316.

Weinstock, J. (1984), Gravity wave saturation and eddy diffusion in the middle atmosphere, *J. Atmos. Terr. Phys.*, *46*, 1069–1082.

Yeh, K. C., and C. H. Liu (1981), The instability of atmospheric gravity waves through wave-wave interactions, *J. Geophys. Res.*, *86*, 9722–9728.

Yu, M. Y. (1999), Some chaotic aspects of the Lorenz-Stenflo equations, *Phys. Scr.*, *T82*, 10–11, doi:10.1238/Physica.Topical.082a00010.

T. W. Garner, Space and Geophysics Laboratory, Applied Research Laboratories, University of Texas at Austin, Austin, TX 78712, USA.

W. Horton, M. L. Mays, and J. W. Van Dam, Institute for Fusion Studies, 1 University Station C1500, University of Texas at Austin, Austin, TX 78712, USA. (horton@physics.utexas.edu)

T. D. Kaladze, I. Vekua Institute of Applied Mathematics, Tbilisi State University, 2 University Street, 0143 Tbilisi, Georgia.